Phys. Status Solidi RRL **9**, No. 2, 125–129 (2015) / **DOI** 10.1002/pssr.201409524

pss +++rapid research letters+++
www.pss-rapid.com

Engineered pixels using active plasmonic holograms with liquid crystals

Calum Williams[*,], Yunuen Montelongo[**], Jaime Oscar Tenorio-Pearl, Andrea Cabrero-Vilatela, Stephan Hofmann, William I. Milne, and Timothy D. Wilkinson**

Electrical Engineering Division, Department of Engineering, University of Cambridge, 9 JJ Thomson Avenue, Cambridge CB3 0FA, United Kingdom

Received 13 October 2014, revised 15 December 2014, accepted 15 December 2014
Published online 12 January 2015

Keywords holography, liquid crystals, optical antennas, pixels, plasmonics

[*] Corresponding author: e-mail cw507@cam.ac.uk
[**] These authors contributed equally.

Digital holography requires arrays of small reconfigurable elements to achieve complex reconstruction of the hologram with common systems based on pixels utilizing liquid crystal on silicon (LCoS) technology. The backplane of a typical pixel element is potentially underutilized and thus relatively large physical areas exist in which information can be stored and exploited to give additional functionality to pixel elements. Polarisation and wavelength dependent optical properties can be achieved in small areas using the plasmonic effects of optical antennae. The integration of LCs with optical antennae-based plasmonic holograms allows active modulation of the far field pattern. The work here demonstrates the concept that conventional LCoS pixel elements can be greatly enhanced with the integration of plasmonic holograms, composed of optical antennae patterned on the surface, giving rise to new levels of modulation capability for holographic pixel elements. Using LCs, polarisation dependent effects in plasmonic holograms can be switched. 'Engineered pixels', with sub-wavelength multiplexing over both polarisation and wavelength, can increase the channel capacity of a typical LC display device.

1 Introduction Holography is an optical technique based on diffraction that encodes information in both the phase and amplitude of light and allows reconstruction of 2D images and 3D objects [1]. In an ideal 3D holographic display element, the optical wavefront can be actively manipulated spatially and temporally [2]. That is, properties of the light field such as phase and amplitude can be modulated. Doing so provides the human eye with all the optical information of the original object leading to full reconstruction. For a digital holographic display, one would require small (diffraction-limited), reconfigurable elements which can locally control the properties of the optical wavefront, in order to represent the complex nature of a hologram [2, 3]. The diffraction process establishes the maximum field of view (FOV) achievable by a pixelated structure obeying Bragg's law, such that 180° FOV reconstruction requires a pixel pitch of at least $\lambda/2$.

State-of-the-art 3D holographic display technologies rely on spatial light modulators (SLMs) ranging from optically addressed, mirror based, to liquid crystal (LC) on silicon (LCoS) devices [4]. To date, LCoS pixel elements in SLMs provide the closest realization to true 3D holography owing to their phase modulation capabilities, performance and scalability [3]. Monochromatic light is diffracted through reconfigurable diffractive elements to form arbitrary field distributions using computer generated holograms (CGHs). Limitations of this technology are: pixel density, pixel pitch, and complex modulation limits. Current attempts to alleviate these problems have been limited due to the fact that most devices have been fabricated for other applications such as data projectors. Some of these devices, such as those being made for the next generation 4k and 8k projectors have pixel densities and pitches which improve holographic applications but are nowhere near the sort required for 3D holography

(~10^{12}–10^{14} pixels required) [5, 6]. The problem is a hologram encodes an enormous amount of optical information and dynamic representation of this requires vast amounts of information modulated on a display device. Furthermore, for an ideal spatial light modulator no technology is capable of achieving LC pixels with size comparable to the wavelength of visible light. The reason is that the electric field deforms the orientation of the LC at the boundaries of the pixel and the need for electrical addressing elements reduces the LC pixel fill-factor [7, 8]. These constraints have prevented its full applicability in holography. The nanoengineering of plasmonic nanostructures may offer a solution to this constrain.

2 Engineered pixels A typical LCoS device consists of a cell fabricated with a parallel pair of electrodes (top and bottom) between which the LC is contained and switched. One of the electrodes is the silicon backplane and the other is a transparent substrate with a conducting layer. The reflective surface is usually polished and covered with a highly reflective Al layer. The surface of the backplane in these devices currently provides no other optical functionality to the pixel itself other than reflecting incident light. Considering the typical available area (~10 μm^2), there is scope for 'engineered' pixel elements in order to expand the functionality of conventional pixels.

Although sub-wavelength holography has been demonstrated for static devices [9], dynamic holography with suitable densities and pitches has only been demonstrated with optically addressable materials [10]. However, electrically reconfigurable holograms with large pixel density remain a challenge. Research has shown that diffraction effects can be controlled by means of plasmonic nanostructures which can propagate optical scattering properties, both in terms of polarization and wavelength dependence, to the far field [9, 11, 12]. Resonant excitations in a localized geometry, termed localized surface plasmon resonances (LSPRs), cause large local electric fields close to the structure surface. Scattering occurs through the excitation of the first order plasmon mode in the metal structure, leading to re-radiation of light, with an array of nanostructures resulting in interference effects. The first order excitation leads to dipolar behavior and, with analogy to macroscopic antenna counterparts, structures of this type are termed optical antennas [13]. For holography, optical antennas provide an interesting alternative to fringes. In these plasmonic holograms, diffraction is produced using the combined plasmonic resonances in arrays of optical antennas and not through the effective behavior of a typical squared pixel or other effective medium approaches [14, 15]. It is therefore possible to multiplex different amplitude and phase CGHs with independent polarization and wavelength dependencies within typical pixel areas [11, 12, 16, 17]. However, these static holograms do not provide any modulation capability post-fabrication. Integration of LCs with metallic nanostructures has been previously demonstrated [18–23], however, these devices mainly provide the functionality for tunable optical filtering in the form of spectrally shifting transmission peaks and operate outside of the visible frequency range in the near to mid-infrared region.

In this Letter, we expand the capabilities of plasmonic holograms by electrically modulating the intensity of the replay field of two independent CGHs encoded on an LCoS backplane. These dynamic diffractive elements are formulated by combining optical antennas with LCs. We propose and demonstrate the potential for increasing the amount of information stored in a typical LCoS pixel made accessible through the patterning of metallic nanostructured elements on a backplane and using LCs to actively select which structures are excited. Moreover, for future display devices, if each pixel were in itself a hologram containing information about an object or pattern, an active backplane array of such 'engineered pixels' could expand the possible information stored in each pixel. For example, integration with fast switching LCs would increase the channel capacity of a display device and moreover the common far field sinc-pattern associated with a conventional pixel may be replaced with something more useful.

3 Design Figure 1 shows the design of the LC plasmonic element ('engineered pixel'). Using nematic LCs above two orthogonal sets of anisotropic Ag optical antennae arrays, the far field pattern corresponding to each array can be selectively constructed by means of an applied switching voltage. Achieved by selecting which antenna's longitudinal LSPR to excite. For nematic LCs aligned 45°

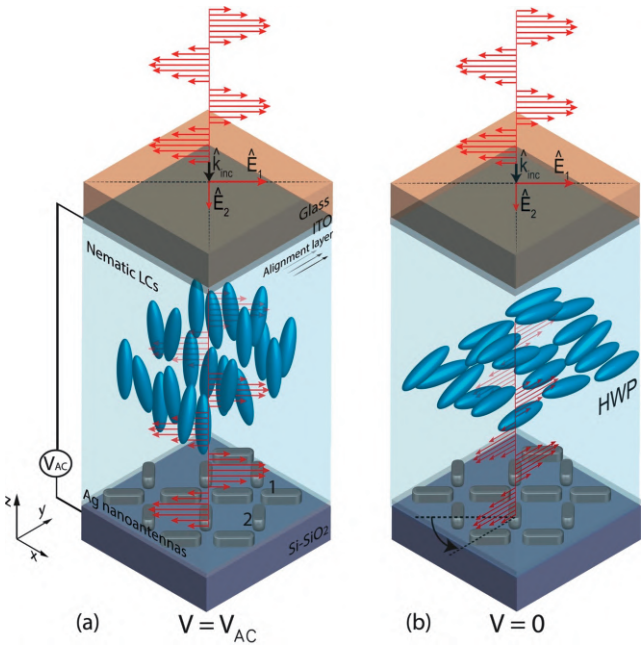

Figure 1 Schematic of liquid crystal optical antennae element on Si showing the switching ability. (a) and (b) State under different voltages. Two sets of orthogonal antennae are used to encode holographic information.

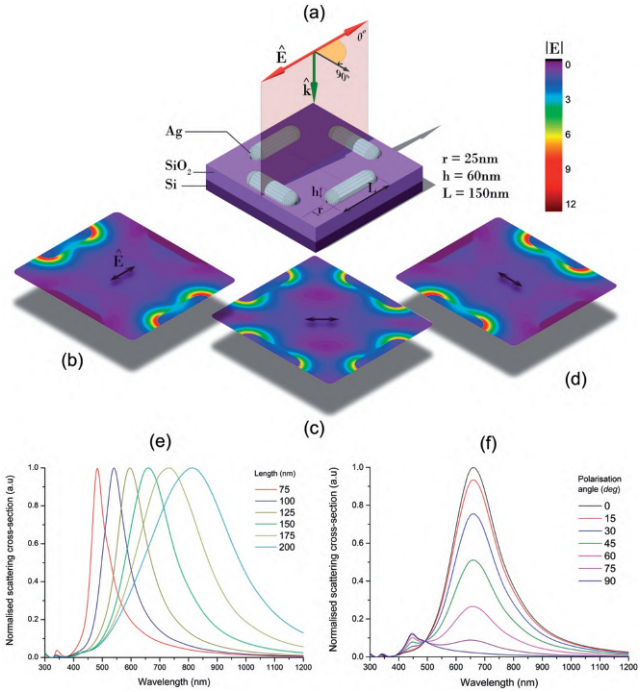

Figure 2 (a) Set-up of the electric field enhancement FDTD simulation of optical antennae on Si. (b–d) show the enhancement under different input polarisation conditions. (e–f) Scattering cross-sections (in a.u.) for the wavelength dependence as a function of antennae length and input polarisation, respectively.

to the antennae in the *x*–*y*-plane, birefringence normal to the plane means it is possible to excite three states: both arrays independently, and an arbitrary superposition of the two. With an applied electric field, the LC molecules are aligned vertically and no birefringence is seen. Polarized light with its electric field parallel to one of the holograms will result in the corresponding image in the far field. When the applied electric field is reduced, the LC molecules rotate and the birefringence of the LC becomes apparent. When the LC layer is acting as a half-wave-plate (HWP), the polarized incident light is rotated by 45° and will additionally excite the second hologram, generating a different replay field.

The switching capability is illustrated in Fig. 2 which shows finite-difference-time-domain (FDTD) simulations [24] of the typical fundamental building block. A set of orthogonal Ag optical antennae (radius 25 nm, height 60 nm and length 150 nm) in a 325 nm unit cell on Si–SiO_2 (200 nm) are excited with 652 nm incident light (a). For polarisation angles 0°, 45° and 90° (b–d), the electric field intensity enhancement is plotted on a plane intersecting the optical antennae at their height midpoint. Strong resonance occurs for parallel electric field components to the antennae. The decomposition of the electric field at 45° into *x*–*y* coordinates means both arrays are excited with equal intensity. The scattering properties of the orthogonal arrays arrangement can be approximated to a single antenna, when the separation is such that the interaction of neighbouring antennas' electric field is negligible. Normalized scattering cross-sections as a function of wavelength and polarisation is shown in (e) and (f), respectively. An anisotropic geometry is chosen to achieve maximum polarisation dependent scattering at 652 nm. The fact that we still see a peak in the blue part of the spectrum under parallel polarisation is indicative of charge oscillations in the transverse mode. This behaviour has been described elsewhere, termed linear wavelength scaling [13, 25].

4 Methods A hologram produced by scattering elements derives from utilizing the field emitted by the nanostructures to create a wavefront reconstruction. The process consists of designing a CGH with the Gerchberg–Saxton algorithm [26], and then sampling scattering elements to produce arbitrary reconstructions [27]. Furthermore, two holograms can be multiplexed for different nanostructures when they are sufficiently uncoupled. In this case we have sampled two independent transverse antennas on a $N \times N$ grid for the two corresponding holograms. These two independent holograms are spatially multiplexed resulting in a wavelength- and polarisation-dependent CGH shown previously in [11, 12]. Hence, two holograms are encoded in the antenna arrays.

The optical antennae are fabricated on top of a polished Si–SiO_2 (200 nm) wafer. Poly-(methyl methacrylate) 950 K resist is spin coated to the wafer and electron beam lithography is used to pattern. After development in a methyl isobutyl ketone/isopropyl alcohol solution (1:3), Ag is thermally evaporated over the sample and lifted off using acetone, yielding a nanostructured backplane. The backplane is coated with LCs aligned 45° to the antennae and sealed with indium tin oxide (ITO) coated glass to form the final cell. The LC was BLO48 standard nematic LC mixture ($\Delta n = 0.25$). The cell gap is 5 μm, with a rubbed AM4276 polyamide alignment layer on the top glass cover only. The 45° alignment layer is used in order for the LCs to act as a half-wave plate for light polarized in the orientation of the respective rods. The fabricated device prior to LC cell construction is shown as an SEM image in Fig. 3. The device is characterized using a low power 652 nm diode laser, with the output polarization controlled using a HWP and two linear polarizers. To increase the apparent brightness of the replay field we focus down to a spot, illuminate the optical antenna based LC-switchable hologram and collect the replay field image on a diffuse sphere in the far field. Control of the hologram's replay field is achieved by applying a voltage to the LCs using the Si and ITO as electrodes. The LC acts as a continuously switchable wave-plate and rotates the electric field incident on the patterned backplane, hence switching between holograms and associated replay fields.

5 Results Figure 4(a) shows the different output states of the device captured using a DLSR camera. The two fabricated holograms encode the Cambridge logo (hologram 1) and Kings College Chapel (hologram 2). State (1)

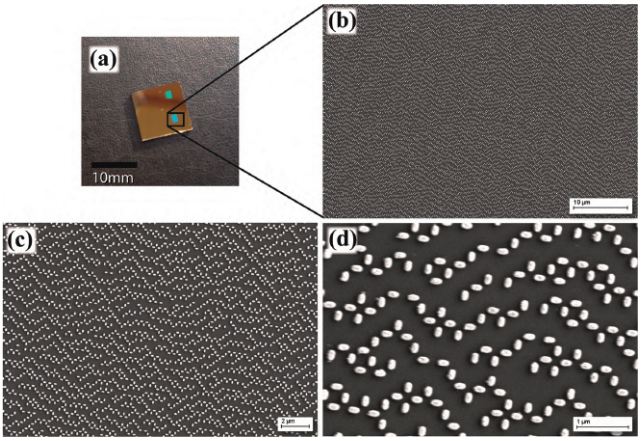

Figure 3 SEM characterization of the fabricated device. (a) Photograph of typical device pre-liquid crystal cell fabrication. (b)–(d) Increasing levels of SEM magnification of the backplane of the device.

is with incident linearly polarized light in the direction of hologram 1 antennae, Fig. 4(b) shows this output at a higher magnification in which the encoded replay field's apodized pixels can be seen. State (1 + 2) is generated through the applied AC bias to the device (5 V at 2 kHz); State (2) is generated through the rotation of incident polarization to align with hologram 2 and again State (1 + 2) is achieved through the AC bias from State (2). The device exhibits wide angle switchable far field capability and demonstrates the ease of integrating optical antennae for wavelength and polarisation effects in LC holographic pixel elements. In comparison to previous work [11, 12] the hologram reconstruction here is controlled entirely with the electrically tunable properties of LCs and not manually through the rotation of the sample or use of additional polarizers. Scaling this to a pixelated backplane matrix would mean each pixel was engineered to encode desired application specific optical information accessible through voltage bias.

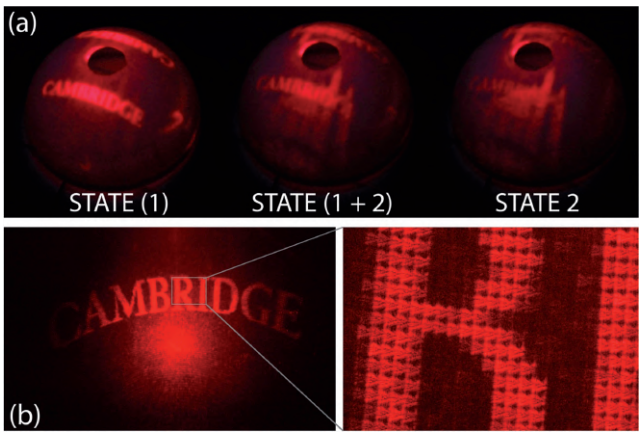

Figure 4 Output states of the final holographic pixel element. (a) The three respective output states with (b) showing state (1) under increased magnification.

Crosstalk between the two states is evident, arising from LC alignment errors resulting in polarisation leakage, and fabrication issues; specifically the 'rounding out' of features meaning enhanced resonance in the transverse mode of the optical antennae. In addition, the interaction of the LCs and antennae may be the possible cause of defects within the device leading to the observed crosstalk. However, the comparison of the two replay field's crosstalk is difficult due to hologram 1 having much higher contrast features in a smaller area than hologram 2.

6 Conclusion We have demonstrated the switching of plasmonic holograms through the integration of liquid crystals in order to form the basis of new types of holographic pixel elements potentially giving increased functionality to a display backplane. Optical antennas on pixel elements can therefore provide polarisation and wavelength dependent control modulated through liquid crystals. By multiplexing over polarisation and wavelength, 'engineered pixels' can increase the channel capacity of a given device. The fabricated device here is compatible with existing semiconductor fabrication processes, and hence the incorporation of such optical antennas on existing LC-based display backplanes to enhance functionality is realistic.

Acknowledgements The authors would like to thank Alexander Macfaden, James Dolan, Ammar Khan, Ananta Palani and Rachel Hyman for their help and support with the research. CW would like to thank the EPSRC Integrated Photonic and Electronic Systems (IPES) Centre for Doctoral Training for their financial support. Y.M., J.O.T.-P, A.C.-V. received financial support from the Cambridge Overseas Trust and the Mexican National Council on Science and Technology.

References

[1] J. Goodman, Introduction to Fourier Optics (McGraw-Hill, New York, 1968).
[2] J. Geng, Adv. Opt. Photon. **5**, 456 (2013).
[3] M. E. Lucente, Electronic Holographic Displays – 20 Years of Interactive Spatial Imaging, in: Handbook of Visual Display Technology, edited by J. Chen, W. Cranton, and M. Fihn (Springer, Berlin, Heidelberg, 2012), Vol. 3, Chap. 9.5.2.
[4] G. Lazarev, A. Hermerschmidt, S. Krüger, and S. Osten, LCOS Spatial Light Modulators: Trends and Applications, in: Optical Imaging and Metrology: Advanced Technologies, edited by W. Osten and N. Reingand (Wiley-VCH, Weinheim, 2012), Chap. 1.
[5] S. A. Benton and V. M. Bove, Holographic Imaging (Wiley, Hoboken, 2008).
[6] M. Lucente, in: SMPTE 2nd Annu. Int. Conf. Stereosc. 3D Media Entertain. – Soc. Motion Pict. Telev. Eng. (2011).
[7] T. D. Wilkinson and R. Rajesekharan, Liquid Crystals for Nanophotonics (Wiley-VCH, Weinheim, 2012), pp. 525–568.
[8] F. Yaras, A. A. Overview, H. Kang, and O. Levent, J. Disp. Technol. **6**, 443 (2010).
[9] N. Yu and F. Capasso, Nature Mater. **13**, 139 (2014).

[10] N. Peyghambarian and S. Tay, Opt. Photon. News **19**, 22 (2008).
[11] Y. Montelongo, J. O. Tenorio-Pearl, W. I. Milne, and T. D. Wilkinson, Nano Lett. **14**, 294 (2014).
[12] Y. Montelongo, J. O. Tenorio-Pearl, C. Williams, S. Zhang, W. I. Milne, and T. D. Wilkinson, Proc. Natl. Acad. Sci. USA **111**, 12679 (2014).
[13] L. Novotny, Phys. Rev. Lett. **98**, 266802 (2007).
[14] W. Yu, K. Takahara, and T. Konishi, Appl. Opt. **39**, 3531 (2000).
[15] S. Larouche, Y. Tsai, T. Tyler, N. Jokerst, and D. Smith, Nature Mater. **11**, 450 (2012).
[16] L. Liu, X. Zhang, M. Kenney, X. Su, N. Xu, C. Ouyang, Y. Shi, J. Han, W. Zhang, and S. Zhang, Adv. Mater. **26**, 5031 (2014).
[17] L. Huang, X. Chen, H. Mühlenbernd, H. Zhang, S. Chen, B. Bai, Q. Tan, G. Jin, K.-W. Cheah, C.-W. Qiu, J. Li, T. Zentgraf, and S. Zhang, Nature Commun. **4**, 2808 (2013).
[18] K. C. Chu, C. Y. Chao, Y. F. Chen, Y. C. Wu, and C. C. Chen, Appl. Phys. Lett. **89**, 103107 (2006).
[19] I. Abdulhalim, J. Nanophoton. **6**, 061001 (2012).
[20] K. Oishi and K. Kajikawa, Opt. Commun. **284**, 3445 (2011).
[21] O. Buchnev, J. Y. Ou, M. Kaczmarek, N. I. Zheludev, and V. A. Fedotov, Opt. Express **21**, 1633 (2013).
[22] N. I. Zheludev and Y. S. Kivshar, Nature Mater. **11**, 917 (2012).
[23] M. Decker, C. Kremers, A. Minovich, I. Staude, A. E. Miroshnichenko, D. Chigrin, D. N. Neshev, C. Jagadish, and Y. S. Kivshar, Opt. Express **21**, 8879 (2013).
[24] FDTD Solutions (Lumerical Solutions Inc., Vancouver, 2013).
[25] F. J. Beck, E. Verhagen, S. Mokkapati, A. Polman, and K. R. Catchpole, Opt. Express **19**, 146 (2011).
[26] R. W. Gerchberg and W. O. Saxton, Optik (Stuttg.) **35**, 237 (1972).
[27] Y. Montelongo, H. Butt, T. Butler, T. D. Wilkinson, and G. A. J. Amaratunga, Nanoscale **5**, 4217 (2013).